Cancer Chemother Pharmacol (2008) 62:985–994
DOI 10.1007/s00280-008-0688-8

ORIGINAL ARTICLE

Non-invasive MRI tumor imaging and synergistic anticancer effect of HSP90 inhibitor and glycolysis inhibitor in RIP1-Tag2 transgenic pancreatic tumor model

Xianhua Cao · Guang Jia · Tao Zhang · Ming Yang · Bing Wang · Peter A. Wassenaar · Hao Cheng · Michael V. Knopp · Duxin Sun

Received: 7 September 2007 / Accepted: 18 January 2008 / Published online: 6 February 2008

Abstract
Purposes To utilize non-invasive MRI imaging for real-time testing the synergistic effects of HSP90 inhibitor and glycolysis inhibitor for pancreatic cancer therapy in spontaneous pancreatic cancer mouse model.
Material and methods Transgenic RIP1-Tag2 spontaneous pancreatic cancer mice were treated with geldanamycin (GA, 5 mg/kg) and /or 3-Bromo-pyruvate (3-BrPA, 5 mg/kg) from 8 to 12 weeks of age. Non-invasive MRI imaging measured and calculated the total tumor mass and volumes in real-time and compared to ex vivo tumors size. Serum VEGF levels were measured by ELISA. HSP 90 client protein levels (AKT and VEGF) were measured by western blots.
Results RIP-Tag2 transgenic mice developed pancreatic tumors from 8 to 12 weeks of age. Non-invasive MRI imaging detected primary tumors in pancreas and metastasis in intestine and mesenterium with minimal resolution of 20 mm^3. VEGF, AKT, hexokinase II, and Hsp90 were expressed in the pancreatic cancer tissues from RIP1-Tag2 transgenic mice. Combination of GA and 3-BrPA decreased serum VEGF levels by 70% compared to control group. Non-invasive MRI imaging showed that combination of GA and 3-BrPA inhibited pancreatic tumor and metastasis by more than 90% and significantly prolonged life span of RIP1-Tag2 transgenic pancreatic cancer mice. The synergistic effect of geldanamycin and 3-BrPA is through inhibition of two different pathways on HSP90 for its client protein degradation and on HK II for energy metabolism.
Conclusion Non-invasive MRI imaging revealed synergistic effects of Hsp90 inhibitors and glycolysis inhibitors, which may provide a new therapeutic option for pancreatic cancer therapy.

Keywords MRI imaging · Synergistic effect · HSP90 inhibitor · Glycolysis inhibitor · Transgenic mice · Pancreatic tumor

Introduction

Pancreatic cancer contributes the fourth leading cause of cancer death in the United States with approximately 30,200 newly diagnosed cases and nearly as many fatalities [1]. The underlying mechanism for the malignance of pancreatic tumor and its high resistance to common therapies are extremely complex. Recently, a number of biochemical and genetic abnormalities have been identified in pancreatic cancer, which include expression of oncogenes (such as K-RAS, AKT) and mutation in tumor-suppressor genes (such as P53), overexpression of growth factors (such as VEGF, EGF) and their receptor (such as EGFR) [2–7]. Due to the complex of the disease, a single molecule which inhibits

Xianhua Cao and Guang Jia have contributed equally to this work.

X. Cao · T. Zhang · B. Wang · H. Cheng · D. Sun (✉)
Division of Pharmaceutics, School of Pharmacy,
Ohio State University, 500 W. 12th Ave.,
Columbus, OH 43210, USA
e-mail: sun.176@osu.edu

G. Jia · M. Yang · P. A. Wassenaar · M. V. Knopp
Department of Radiology, The Ohio State University,
Columbus, OH 43210, USA

Present Address:
X. Cao
Drug Discovery Support, Boehringer Ingelheim Pharmaceutical Inc., 900 Ridgebury Rd., P.O. Box 368, Ridgefield,
CT 06877, USA

one specific target is unlikely to be effective for pancreatic cancer therapy. In such case, HSP90 inhibitors provide a new hope for pancreatic cancer therapy by inhibiting the function of chaperone HSP90 and simultaneously down regulating many oncogenic proteins.

In addition, a vast majority of tumors display a high rate glycolysis, a phenomenon known as the Warburg effect [8, 9]. Cancer cells often switch glucose metabolism from tricaboxylic acid (TCA) cycle to anaerobic glycolysis for ATP production [10, 11]. However, anaerobic glycolysis only produces two molecules of ATP, while TCA produces 38 molecules of ATP from each glucose molecule. Thus, complete loss of TCA cycle for ATP production would result in a 19-fold increase in glucose consumption in cancer cell for the energy needs. High rate glycolysis is associated with high level of glucose transporters [12], hexokinase, and lactate dehydrgenase A [13].

Indeed, high rate glycolysis is validated by clinical used tumor imaging technique—positron emission tomography (PET). PET utilizes high rate of glycolysis in tumors to produce cancer images using 2-[^{18}F] fluoro-2-deoxy-D-glucose (FDG) as a tracer. Since a fundamental characteristic of malignant tumors is increased glucose uptake and glycolysis [8, 14, 15], much more FDG is transported into the tumor cells by high levels of glucose transporters [16–21]. Subsequently, FDG is phosphorylated inside the cells by hexokinases at C-6 position to form FDG-6-phosphate. FDG-6-phosphate can neither be further metabolized nor exported outside of the cells, and thus is trapped inside of cells for tumor imaging [22, 23]. These data indicate that high rate glycolysis is the survival mechanism for cancer cells. Therefore inhibition of glycolysis in cancer may provide a therapeutic regimen for solid tumor.

In this report, the first aim is to determine the synergistic in vivo antitumor effects of HSP90 inhibitor (galdanamycin, GA) in combination with glycolysis inhibitor in RIP1-Tag2 transgenic pancreatic cancer mice model. HSP90 inhibitor will inhibit the function of chaperone HSP90 to downregulate many oncogenic proteins simultaneously. Due to the dependency on high glycolysis rate in pancreatic tumor, we hypothesize that glycolysis inhibitor (3-Bromopyruvate, 3-BrPA) will selectively sensitize the anticancer effect of HSP90 inhibitor in RIP1-Tag2 pancreatic cancer model.

In RIP1-Tag2 transgenic pancreatic cancer model, the rat insulin promoter 1 (RIP1) directs the expression of the simian virus 40 large T antigen 2 (Tag2) in pancreatic beta cells and induces multistage carcinogenesis [24]. From 4 to 7 weeks of age, a VEGF involved angiogenic switch activates the quiescent vasculature and promotes angiogenesis in hyperproliferative lesions in the positive transgenic mice, characterized by endothelial cell proliferation, dilated blood vessels, and microhemorrhage [25–27]. Solid tumors and metastasis emerge at about 8–12 weeks in pancreas and mesenterium. This model has provided a good preclinical spontaneous pancreatic tumor model for testing experimental therapeutics.

The wide spread use of new orthotopic models with deep seated tumors require the use of in vivo imaging methods to serially monitor treatment regimens. Therefore, the second aim of this research is to establish a non-invasive dynamic magnetic resonance imaging (MRI) imaging method to monitor the tumor growth and synergistic anticancer effect of HSP90 inhibitor and glycolysis inhibitor in RIP1-Tag2 pancreatic cancer model.

The non-invasive small-animal imaging has become an area of interests in order to effectively and dynamically image and monitor the disease process and therapeutic regimen in real time. Various imaging methods have been evaluated in animal model. Magnetic resonance imaging [28] and positron emission tomography with radioactive tracer [29] were implemented to evaluate the tumors in pancreatic cancer xenograft model. Optical near infrared imaging [30] and red fluorescent protein imaging [31], were used for orthotopic model of pancreatic cancer. Pinhole SPECT/CT with a ligand for glucagons-like peptide-1 receptor were evaluated to detect the tumors in RIP1-Tag2 mice [32]. This study investigated the possibility of a novel MRI imaging method to assess pancreatic tumor development in real-time from 8 to 12 weeks in RIP1-Tag2 transgenic pancreatic cancer mice model.

Materials and methods

Cell culture, reagents, and antibodies

Human pancreatic cancer cell lines BxPC3 were used in the in vitro mechanism study and cultured by 10% FBS RPMI-1640 at 37°C and 5% CO_2. All the antibodies for immunohistochemistry or western blots analysis were bought from Cell Signaling Technology except hexokinase II antibody from Chemicon International. VEGF Elisa kit was bought from R and D systems. The glycolysis inhibitor 3-BrPA was bought from Sigma-Aldrich.

Transgenic mice

RIP1-Tag2 transgenic mice of a C3/Cg background contains the insulin promoter-driven SV40 Large T antigen and produce spontaneous multifocal and multistage pancreatic islet solid tumors [24]. RIP1-Tag2 positive mice were selected with genotyping from tail-tip DNA by PCR. The primer sequences has been previously reported as GGACA AACCACAACTAGAATGCAGTG/CAGAGCAGAATTG TGGA-GTGG [33]. Positive RIP1-Tag2 transgenic mice

between 7 and 12 weeks of age were used in these studies. Mice were housed under barrier conditions at the animal care facility at the Ohio State University, Columbus, Ohio. The Institutional Animal Care and Use Committee (IACUC) at The Ohio State University approved all experimental procedures.

In vivo antitumor treatment and tumor monitoring

Positive RIP1-Tag2 transgenic littermates were randomized into different groups for single treatment or combination treatment of 5 mg/kg geldanamycin (GA) and 5 mg/kg 3-BrPA. All compounds were freshly prepared and injected intraperitoneally twice per week for 5 weeks from the 8 weeks of age. At 12 weeks of age all animals underwent careful and extensive autopsies of the pancreas and abdominal cavities. The total tumor mass were weighed and total volumes were added up with each single tumor volume measured with a caliper and calculated as: single tumor volume = 0.5 × (length × width^2). The serum was collected and stored at −80°C for VEGF Elisa analysis. Tumor tissues were either subjected to immunohistochemistry analysis.

Immunohistochemistry (IHC)

The methods for immunohistochemistry have been described previously [34]. Briefly, tissues were fixed by 4% paraformaldehyde for 6–12 h and paraffin-embeded. Slides were counterstained in Richard Allen hematoxylin, dehydrated through graded ethanol solutions and cover-slipped. VEGF primary antibody was used at a dilution of 1:50, HSP90 antibody at a dilution of 1:250, hexokinase II at a dilution of 1:500, and p-AKT(Ser473) antibody at a dilution of 1:100. Primary antibodies were incubated for one hour for VEGF and hexokinase II and overnight for HSP90 and p-AKT. The detection system used was a Labeled Streptavidin-Biotin Complex. This method is based on the consecutive application of (1) A primary antibody against the antigen to be localized; (2) biotinylated linking secondary antibody against primary antibody; (3) peroxidase conjugated streptavidin to bind to biotin; and (4) enzyme substrate chromogen (DAB) for detection. The positive and negative controls stained appropriately.

Western blot analysis

Tumor Tissues were washed twice with phosphate-buffered saline (PBS), homogenized in lysis buffer (50 mM PH 7.6 Tris–HCl, 250 mM NaCl, 5 mM EDTA, 2 mM Na_3VO_4, 50 mM NaF) with 1% protease inhibitor cocktail (P8340, Sigma) on ice, and then sonicated three times for 20 sec. Supernatants were collected after 10 min centrifuge (15,000 rpm) at 4°C. Protein concentration was determined using BCA protein assay method (PIERCE). The samples were incubated with 2 × SDS loading buffer and boiled for 5 min. Then 30 μg of total protein was subjected to electrophoresis and separated in 10% SDS-polyacrylamide gels (Bio-Rad), transferred to nitrocellulose filters, probed with the antibodies of interest, and developed by enhanced chemiluminescence system ECL (Amersham).

Non-invasive in vivo tumor image by MRI

From 8 weeks of age, all mice were monitored by a 3 Tesla clinical MRI system (Achieva, Philips Medical Systems) for tumor growth and therapeutic effect of geldanamycin and 3-BrPA. Briefly, 200 μl of 0.01 M extracellular contrast agent contrast agent gadobutrol (Gd-BT-DO3A, Gadovist; Schering AG, Berlin, Germany) was orally administrated 5 min before anesthesia. The animals were scanned in a prone position, using a dedicated mouse coil (Philips Research laboratory). T2-weighted coronal images were obtained using a Turbo Spin Echo (TSE) sequence (TR/TE = 8,708/77 ms, field of view = 60 × 60 mm^2, matrix = 512 × 512 with in plane resolution 0.12 × 0.12 mm^2, number of excitations = 1, 26 slices, 1 mm slice thickness, contiguous slices without gap). From the images, the stomach and gut in the mice were found with rounded shape due to the filling of the contrast agent, which effectively suppressed the motion artifacts affecting the imaging results. No further motion correction was implemented in the image post-processing. The image post-processing including tumor segmentation and 3-dimensional visualization was carried out using the MIPAV (Medical Image Processing, Analysis, and Visualization) software from NIH (http://mipav.cit.nih.gov/). The calculated tumor sizes from MRI were correlated to those measured tumor volumes ex vivo.

Data analysis

Data are mean ± SD. Student's *t* test or ANOVA test were used for statistical analyses.

Results

Pancreatic tumor development in RIP1-Tag2 transgenic mice

In order to select the positive transgenic mice for combination treatment of HSP90 inhibitor and glycolysis inhibitor, the mice were genotyped for detection of RIP1-Tag2 transgene at 2–3 weeks of age. Figure 1 (up panel) shows the PCR results of the genotyping. Positive transgenic mice

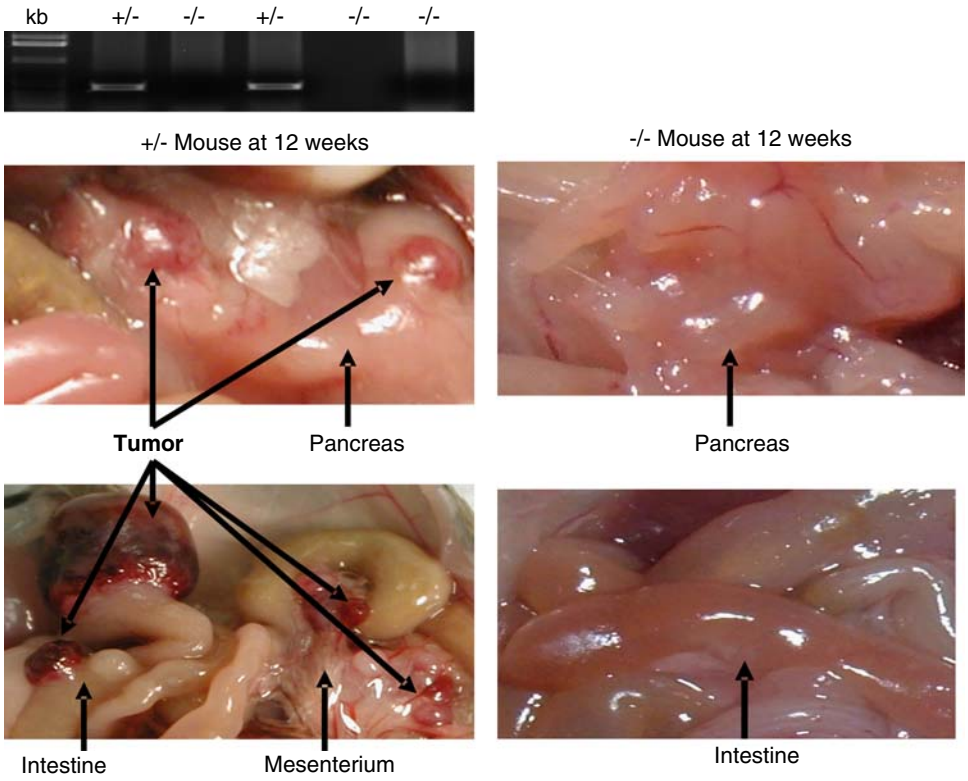

Fig. 1 Spontaneous pancreatic tumor and metastasis in RIP-Tag2 transgenic mice at 12 weeks [transgenic expression of SV40 large T antigen (TAg) under rat insulin promoter]

have a band at 450 bp while normal mice show clear background in the 2% Agarose gel. To further confirm the pancreatic tumor in RIP1-Tag2 transgenic mice, the in situ pancreas tissue and intestine were intensively explored after the mice were sacrifice at the age of 12 weeks. As shown in Fig. 1 (middle and low panel), solid tumors appeared in the pancreas and metastasis was found in both intestine wall and mensenterium in RIP1-Tag2 transgenic mice.

Expression of HSP90, VEGF, PiAKT, and Hexokinase II (HKII) in pancreatic tumors of RIP1-Tag2 transgenic mice

Histology and immunohistochemistry were further conducted to identify the characteristics of pancreatic tumor in RIP1-Tag2 transgenic mice. Figure 2 shows the high expression level of HSP90, VEGF, PiAKT and HK II expression level in solid tumors at age of 12 weeks. VEGF is the critical factor involved in the angiogenesis during tumor progression, AKT plays an important role in the tumor survival regulation, HKII is one of the most important energy metabolism enzymes in solid tumors. These proteins are directly related to tumor development and metastasis stage. Thus simultaneously targeting multiple proteins and inhibiting the tumor energy sources at the same time provide a potential therapeutic regimen for pancreatic tumor.

Synergistic antitumor effect of HSP90 inhibitor and glycolysis inhibitor in RIP1-Tag2 transgenic pancreatic tumor mice

Geldanamycin inhibited the function of molecular chaperone of HSP90 to simultaneously down-regulate many oncogenic proteins including VEGF and AKT. Our previous studies have proven that a hexokinase II inhibitor (3-Bromo-pyruvate, 3-BrPA) inhibited the glycolysis rate in cancer cells (Cao X et al. unpublished data). In order to test the synergistic effect of HSP90 inhibitor and glycolysis inhibitor in RIP1-Tag2 transgenic pancreatic cancer mice, 3-BrPA (5 mg/kg, twice/week) and GA (5 mg/kg, twice/week) were combined to treat positive RIP1-Tag2 transgenic mice from 8 to 12 weeks of age. The total tumor mass and volume, in situ tumor metastasis and VEGF amount in serum were compared to either non-treatment mice or single treatment mice with GA or 3-BrPA alone.

As shown in Fig. 3a, without any treatment, the RIP1-Tag2 transgenic mice had over 250 mm^3 total tumor volume and 300 mg total tumor mass at the 12 weeks of age. Single treatment with either GA (5 mg/kg) or 3-BrPA (3 mg/kg) had no effects or minimal effects on tumor growth compared with the control groups. However, combination treatments with GA (5 mg/kg) and 3-BrPA (5 mg/kg) in these transgenic mice showed 90% inhibition on the tumor development, with only 20 mm^3 total

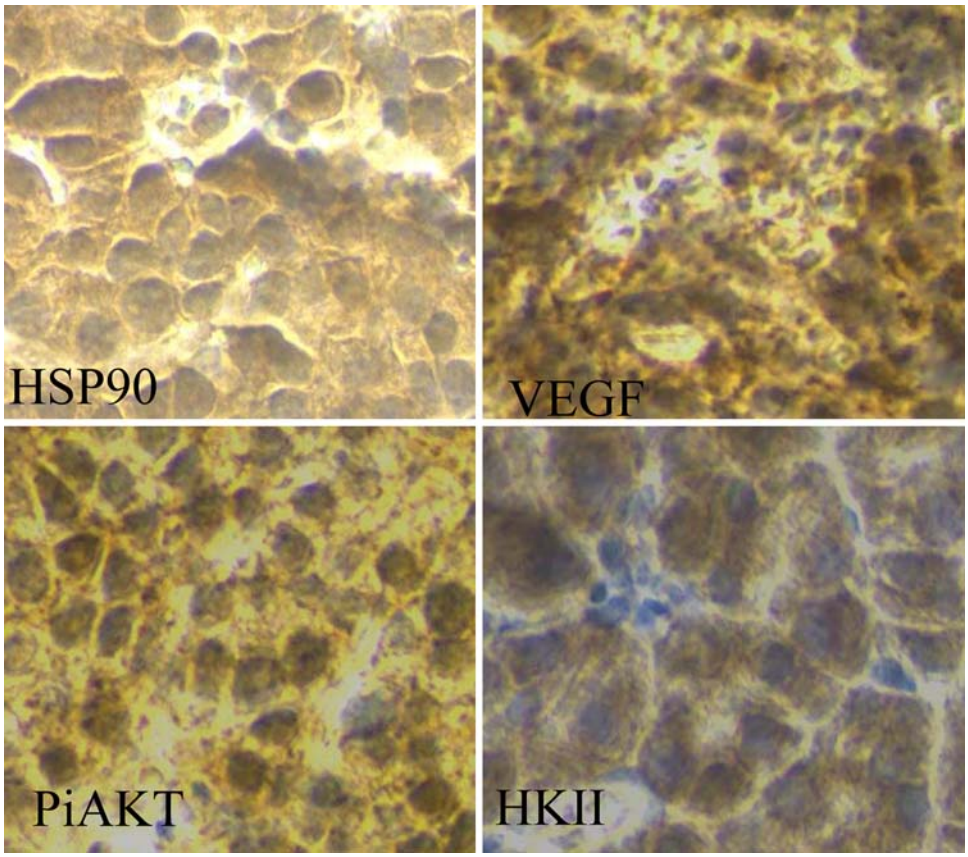

Fig. 2 High expression of HSP90, VEGF, Pi-AKT, and Hexokinase II (HKII) in pancreatic tumor tissues of RIP1-Tag2 transgenic mice. The tumor tissues are fixed in formalin and then paraffin embedded for section. VEGF primary antibody was used at a dilution of 1:50, HSP90 antibody at a dilution of 1:250, hexokinase II at a dilution of 1:500, and p-AKT(Ser473) antibody at a dilution of 1:100

tumor volume and 20 mg total tumor mass at the 12 weeks of age.

The analysis of in situ tumor and ex vivo tumors were further confirmed in Fig. 3b for the synergistic antitumor effect of GA and 3-BrPA. The metastasis were developed in both the intestine or mensenterium in the single treatment and control groups, while much smaller tumors were detected only on pancreas in the combination treatment group with GA and 3-BrPA (Fig 3b). This suggests that simultaneously inhibiting HSP90 and glycolysis significantly inhibit the metastasis and tumor growth in RIP1-Tag2 transgenic pancreatic cancer mice.

Previous study reported that VEGF was elevated in RIP1-Tag2 transgenic pancreatic cancer mice [35, 36]. Therefore, we tested the in vivo effects of HSP90 inhibitor GA and glycolysis inhibitor 3-BrPA for the serum VEGF concentration in either single treatment or combination treatment groups. As illustrated in Fig. 3c, control mice (RIP1-Tag2 transgenic mice without treatment) showed significant higher level (3-fold) of serum VEGF compared to the littermate normal mice (no RIP1-Tag2 transgene). Combinational treatment of GA and 3-BrPA completely inhibited the VEGF production by 70% in RIP1-Tag2 transgenic mice to the normal level similar to normal littermate mice (without RIP1-Tag2 transgene) while single treatment with GA or 3-BrPA exhibited minimum inhibition of VEGF production by 20–40%.

MRI non-invasive imaging pancreatic tumors in RIP1-Tag2 transgenic mice

In order to monitor the tumor development rate and confirm the synergistic anticancer activity of combination treatment of GA and 3-BrPA in vivo, we developed a non-invasive MRI imaging method for the pancreatic tumor in the transgenic RIP1-Tag2 mice. Figure 4 showed the non-invasive MRI images of the positive transgenic mice at end of the experiments. This non-invasive MRI imaging detected not only the pancreatic tumors (lower panel in Fig. 4) but also the metastatic tumors (up panel in Fig. 4). The predicted tumor volume and status by non-invasive MRI correlated with the measured tumor size ex vivo (left columns in Fig. 4). This non-invasive MRI imaging detected the small tumor lesions at 20 mm^3. These data indicate that the non-invasive MRI imaging method is able to detect the pancreatic tumor development rate in real time in RIP1-Tag2 transgenic mice from week 8 to week 12. The non-invasive tumor imaging provides a feasible way to quantify the therapeutic efficacy of the combination treatment of Hsp90 inhibitor and glycolysis inhibitor.

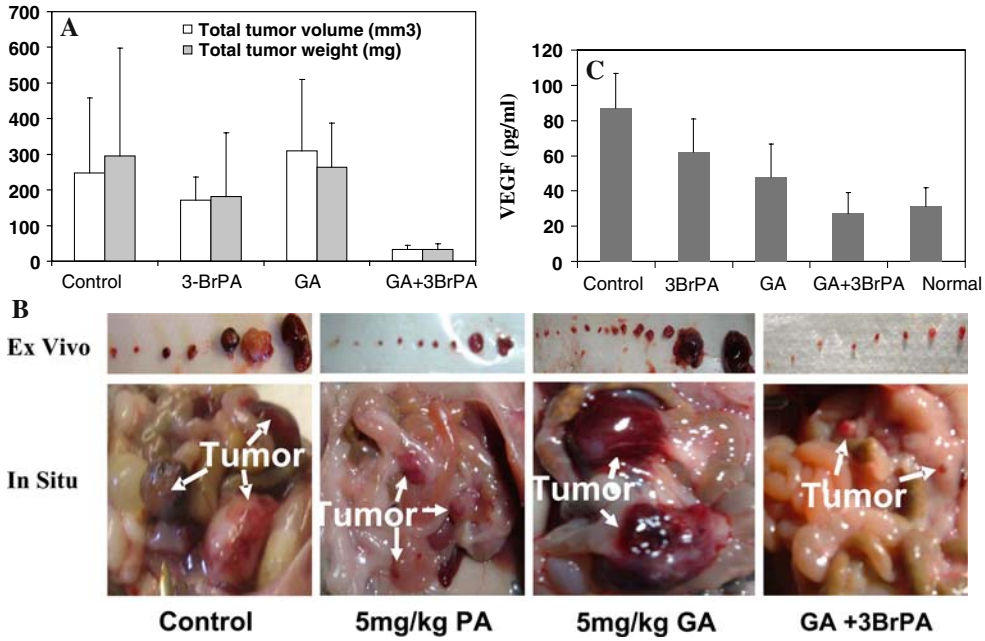

Fig. 3 **a** Total tumor volume and tumor mass in both pancreas and metastasis in mesenterium. Mice were treated with GA (5 mg/kg) or 3-BrPA (5 mg/kg) alone or in combination from week 7 to week 11. The mice were sacrificed at week 12 to measure the tumor volume and tumor mass. $n = 5$. **b** Representative image of spontaneous pancreatic tumor and metastasis in intestine and mesenterium in RIP1-Tag2 transgenic mice at 12 weeks of age after drug treatment with geldanamycin (GA, 5 mg/kg) or/and 3-BrPA (5 mg/kg). **c** Serum VEGF levels in RIP1-Tag2 transgenic pancreatic cancer mouse model (with drug treatment of GA 5 mg/kg, or/and 3-BrPA 5 mg/kg) and littermate normal mice (Normal). $n = 5$

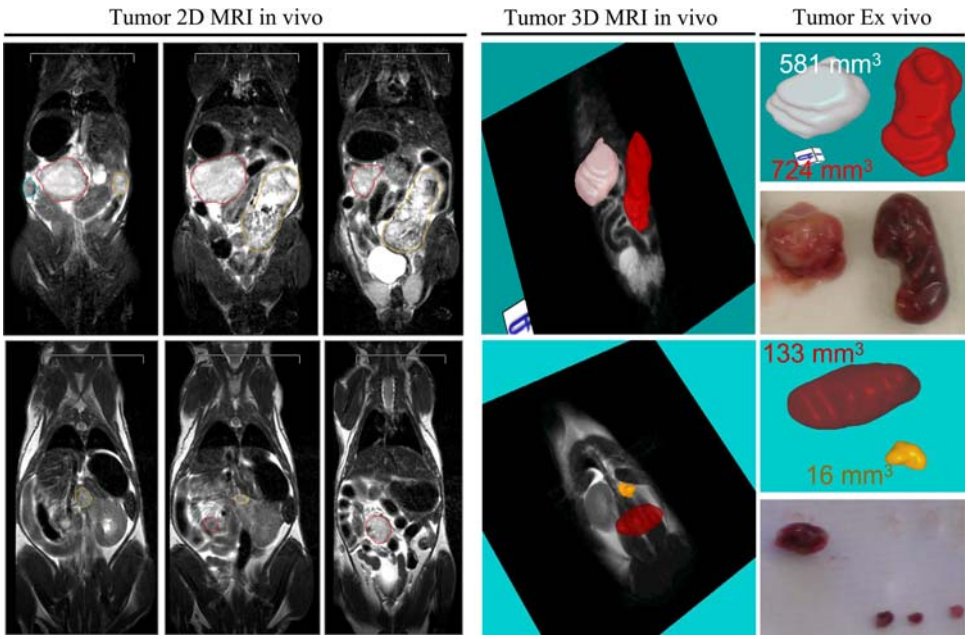

Fig. 4 Non-invasive MRI imaging of pancreatic tumors and metastasis in RIP1-Tag2 pancreatic mouse model in vivo compared to tumor size ex vivo

Non-invasive MRI imaging showed that combination of Hsp90 inhibitor and glycolysis inhibitor significant inhibited pancreatic tumor growth from week 8 to week 12 in RIP1-Tag2 transgenic mice

In vivo pancreatic tumor growth rate from week 8 to week 12 of RIP-Tag2 was measured in real-time by the non-invasive MRI tumor imaging during the combination treatment of Hsp90 inhibitor and glycolysis inhibitor. The various treatment regimen was blind to MRI specialist for MRI imaging. The tumor size was calculated by the non-invasive MRI images and the total tumor volumes were normalized to the tumor volumes at 8 weeks of age before treatment. Figure 5a shows the 2-dimensional and

3-dimensional non-invasive MRI images in both control group and combination treatment group from week 8 to week 12. The 3-dimensional MRI images indicated that the tumor growth rate was significantly inhibited in the combination treatment by more than 90% when compared to the non-treatment group. As shown in Fig. 5b, the average of total tumor volumes in the control group were grown 2-fold bigger at the 12 weeks of age than the initial volumes at 8 weeks of age. Significantly, the combination of geldanamycin (GA) and 3-BrPA in transgenic mice showed more than 90% inhibition on the tumor growth at the 12 weeks of age, with only 1.1–1.2 fold of the initial tumor volumes at 8 weeks of age.

Combination treatment of geldanamycin (GA) and 3-BrPA enhanced mouse survival in RIP1-Tag2 transgenic pancreatic tumor mice

RIP1-Tag2 transgenic pancreatic cancer mice have a very short life span of 10–12 weeks due to the pancreatic tumor burden. In order to verify whether the synergistic inhibition of tumor growth by combination treatment of GA and 3-BrPA can prolong the life span in RIP1-Tag2 transgenic mice, the survival rates were further analyzed during various treatments. As illustrated in Fig. 6, the median survival time in combination treatment group (GA and 3-BrPA) was significantly delayed to over 95 days ($P < 0.05$ vs. control), while the median survival time in control group was ~83 days. In contrast, neither single 3-BrPA treatment group nor single GA treatment group showed significant survival benefits with the median survival time of 83.5 days ($P = 0.87$ vs. control) and 88 days ($P = 0.67$ vs. control), respectively.

Combination of GA and 3-BrPA exhibited better anticancer effect in pancreatic cancer cells through induction of Hsp90 client protein degradation

To further explore the mechanism of synergistic antitumor effect of the combination treatment of GA and PA, We evaluated the mechanism for the combination of geldanamycin and 3-BrPA in pancreatic cancer cells (BxPC-3) in vitro. MTS assay was used to measure the cell viability. Western blot was used to measure the HSP90 client proteins levels after drug treatment. The results showed that the combination of GA and 3-BrPA increased cytotoxicity by more than 3-fold (Cao X et al. unpublished data). As shown in Fig. 7, GA alone induced multiple client proteins degradation (AKT, VEGF, HKII) by 40 to 50% in pancreatic cancer cells (BxPc-3). Combination treatment by GA and 3-BrPA enhanced the degradation of AKT to 60%. HSP90 level was not altered by the drug treatment. These data suggest that synergistic effect of GA and 3-BrPA is through inhibition of two pathways on Hsp90 for its client protein degradation and on HK II for energy metabolism.

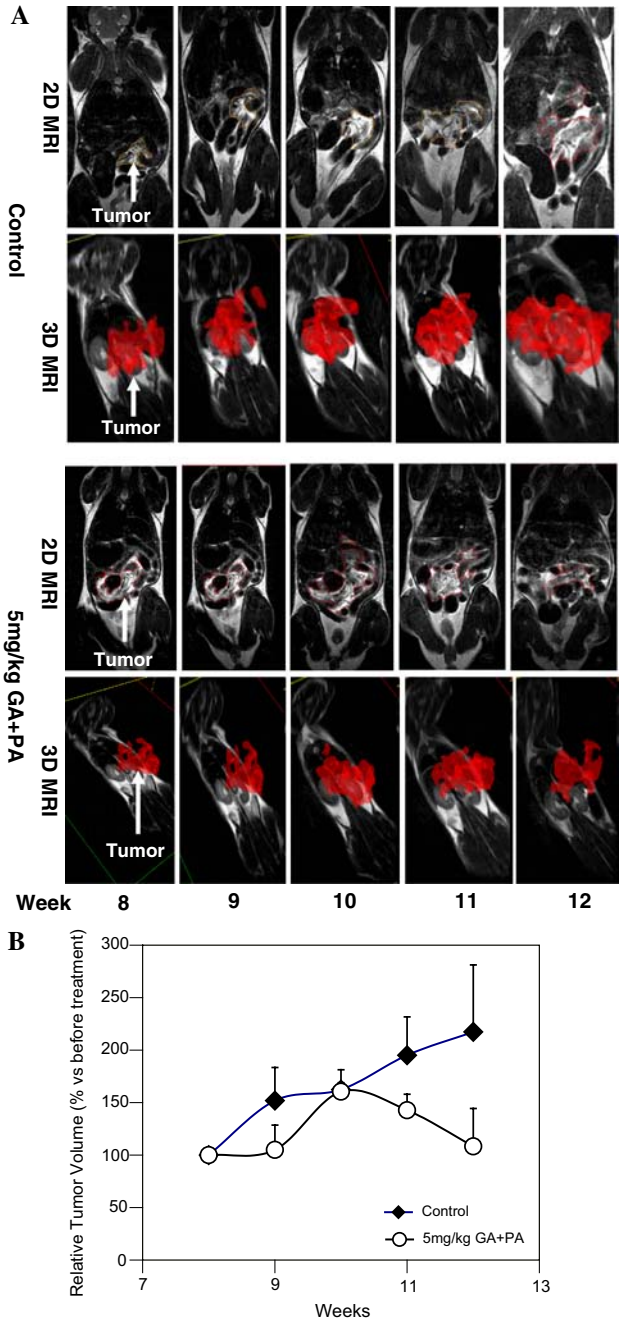

Fig. 5 **a** Representative Non-invasive MRI imaging to detect tumor development and therapeutic efficacy of combination of GA (5 mg/kg) and 3-BrPA (5 mg/kg) in real time in RIP1-Tag2 transgenic pancreatic cancer mouse model from 8 to 12 weeks of age. **b** Non-invasive MRI imaging calculated tumor volume in RIP1-Tag2 transgenic pancreatic cancer model to measure the tumor development and therapeutic efficacy of GA (5 mg/kg) and 3-BrPA (5 mg/kg) in real time from 8 to 12 weeks of age. $n = 5$

Discussion

Many clinical trials failed to demonstrate therapeutic benefits using single agent to target single oncogenic protein or

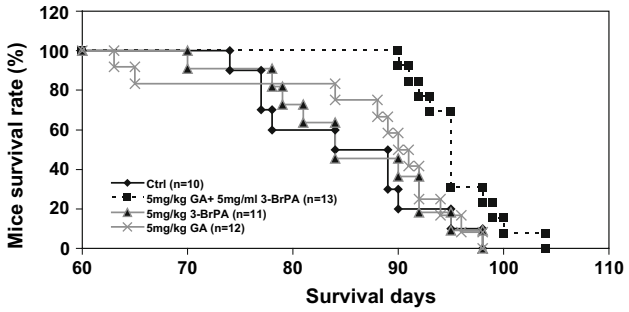

Fig. 6 Survival rate of Rip1-Tag2 transgenic pancreatic cancer mice after drug treatment with GA (5 mg/kg, $n = 12$), 3-BrPA (5 mg/kg, $n = 11$), and combination of GA and 3-BrPA ($n = 13$) compared to control ($n = 10$)

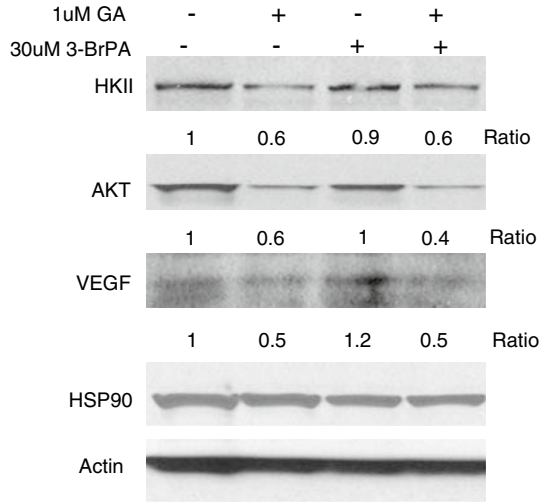

Fig. 7 Western blot detects levels of HSP90 client proteins after drug treatment in pancreatic cancer cells (BxPC-3). Actin was used to normalize each band. Ratio is calculated by comparison of the normalized band in treatment group versus control group

angiogenesis in pancreatic tumors [37–39). This may due to the fact that pancreatic cancer cells have a large number of biochemical and genetic abnormalities including overexpression of HIF-1α, HSP90, AKT, Erb2, VEGF, and EGFR in addition to the mutation of many oncogenes or tumor suppressor genes such as K-Ras, P16, P53, and BRAC2 [6, 7, 40–44]. All these abnormally triggered-signaling cascade alterations have made pancreatic cancer highly resistant to therapies. HSP90 inhibitors provide a hope for therapy of pancreatic cancer by inhibiting molecular chaperone Hsp90 and simultaneously down-regulate many oncogenic proteins. Our previous studies have proven that inhibiting ATP-dependent chaperone activity of HSP90 by GA in combination with glycolysis inhibitor have higher anticancer efficacy and more potent induction of HSP90 client proteins in both in vitro and in vivo pancreatic tumor xenograft models (Cao X et al. unpublished data). In this study, we report the synergistic antitumor effects of HSP90 inhibitor and glycolysis inhibitor in RIP1-Tag2 transgenic pancreatic tumor mice.

Angiogenesis plays an important role during carcinogenesis of solid tumors and invasive carcinoma in RIP1-Tag2 transgenic pancreatic tumor mouse model. VEGF is one of the important pro-angiogenic factors that mediated the angiogenic switch during tumor progress in these mice [25, 36]. Conditional inhibiting the VEGF expression has been reported to block the tumor angiogenesis efficiently and tumor outgrowth [36]. HSP90 inhibitors modulate multiple functions required for tumor angiogenesis [45]. Our combination study with GA decreased the VEGF levels both in vitro and in vivo. Combination of GA and glycolysis inhibitor 3-BrPA shows significant ablation of VEGF in RIP1-Tag2 transgenic mice (Fig. 3c) and has the synergistic inhibition of the tumor progression (Fig. 3a, b).

The mechanism studies in cancer cells in vitro further confirmed the synergistic anticancer effects by exploring the degradation of HSP90 client proteins during combination treatment of GA and 3-BrPA (Fig. 7). Through the inhibition of molecular chaperon function of HSP90 by geldanamycin, not only VEGF was degraded but also other oncogenic proteins such as AKT. In addition, pancreatic cancer highly depends on the high rate of glycolysis to provide the energy sources to maintain the proliferation rate of the cancer cells [46, 47]. Further inhibition of the hexokinase II function for energy metabolism in pancreatic cancer cells by 3-BrPA cause more VEGF and AKT degradation. Thus, combination treatment with HSP90 inhibitor and glycolysis inhibitor may provide a more efficacious therapeutic option than the classic angiogenesis inhibitor alone in anticancer therapy.

Xenograft mouse model is widely used to assess therapeutic regimen for anticancer therapy for its easily controlled tumor growth monitoring. However, orthotopic tumor models are taking their advantages with closer imitation to clinical tumor characteristics. These new orthotopic models with deep seated tumors require the use of in vivo imaging methods to assess therapeutic regimen in stead of sacrificing the animals. In our study, we utilized a spontaneous pancreatic tumor model (RIP1-Tag2) to evaluate combination therapy of HSP90 inhibitor and glycolysis inhibitor. To overcome the shortcomings of the monitoring of tumor growth in pancreas and its metastasis in this spontaneous pancreatic cancer model, we developed a non-invasive MRI imaging method to detect the tumorgenesis and monitor the tumor development rate in real-time from week 8 to week 12. In RIP1-Tag2 transgenic pancreatic cancer mouse model, the pancreatic cancer arises from normal beta-cells in their natural tissue microenvironments and progresses through multiple stages to invasive carcinoma. Metastasis is detected in the nearby intestine and mesenterium in the late stage of positive transgenic mice, which is

similar to human pancreatic tumor. Using non-invasive MRI imaging, the pancreatic tumors mass and volume and the real-time tumor development can be easily detected. In our method, the contrast agent was orally given and distributed in the stomach and intestine, which provided dark signal in the T2-weighted images. The border of the stomach and intestine was then delineated, and pancreatic tumor and metastasis were clearly detected. The tumor progression rate in different treatment strategies is monitored in real time to directly reflect the therapeutic efficacy. Our non-invasive MRI images during the combination treatment of GA and 3-BrPA showed more than 90% inhibition, which is correlated to the ex vivo tumor measurement (Figs. 5, 3). The limitation of the study is lack of tumor analysis using RECIST criteria [48] due to low image resolution. In addition, the mice in week 8 mainly had nonmeasurable small lesions, making it difficult to use RECIST criteria. Further studies with improved image resolution will include RECIST criteria for tumor measurement.

In summary, combinational treatment of HSP90 inhibitor and glycolysis inhibitor showed synergistic antitumor efficacy in RIP1-Tag2 transgenic pancreatic tumor mice from 8 to 12 weeks of ages. The synergistic effect of this combination therapy is through inhibition of two pathways on HSP90 for its client protein degradations (VEGF, AKT, and HKII) and on HK II for energy metabolism. Non-invasive MRI imaging was developed to monitor the tumor growth and therapeutic efficacy in real time in RIP1-Tag2 transgenic pancreatic model. The non-invasive MRI imaging confirmed that GA and 3-BrPA inhibit more than 90% tumor growth rate. The combination of geldanamycin and 3-BrPA also significantly prolonged the life span of RIP1-Tag2 transgenic pancreatic cancer mice. Therefore, HSP90 inhibitors in combination with glycolysis inhibitors may provide a new therapeutic option for pancreatic cancer therapy.

References

1. Parker SL, Davis KJ, Wingo PA, Ries LA, Heath CW Jr (1998) Cancer statistics by race and ethnicity. CA Cancer J Clin 48:31–48
2. Li D, Xie K, Wolff R, Abbruzzese JL (2004) Pancreatic cancer. Lancet 363:1049–1057
3. Spratlin J, Sangha R, Glubrecht D, Dabbagh L, Young JD, Dumontet C, Cass C, Lai R, Mackey JR (2004) The absence of human equilibrative nucleoside transporter 1 is associated with reduced survival in patients with gemcitabine-treated pancreas adenocarcinoma. Clin Cancer Res 10:6956–6961
4. Laheru D, Biedrzycki B, Jaffee EM (2001) Immunologic approaches to the management of pancreatic cancer. Cancer J 7:324–337
5. Pardoll D, Allison J (2004) Cancer immunotherapy: breaking the barriers to harvest the crop. Nat Med 10:887–892
6. Buchler P, Reber HA, Buchler M, Shrinkante S, Buchler MW, Friess H, Semenza GL, Hines OJ (2003) Hypoxia-inducible factor 1 regulates vascular endothelial growth factor expression in human pancreatic cancer. Pancreas 26:56–64
7. Ghaneh P, Kawesha A, Evans JD, Neoptolemos JP (2002) Molecular prognostic markers in pancreatic cancer. J Hepatobiliary Pancreat Surg 9:1–11
8. Warburg O (1956) On the origin of cancer cells. Science 123:309–314
9. Gatenby RA (1995) The potential role of transformation-induced metabolic changes in tumor-host interaction. Cancer Res 55:4151–4156
10. Dang CV, Semenza GL (1999) Oncogenic alterations of metabolism. Trends Biochem Sci 24:68–72
11. Seagroves TN, Ryan HE, Lu H, Wouters BG, Knapp M, Thibault P, Laderoute K, Johnson RS (2001) Transcription factor HIF-1 is a necessary mediator of the pasteur effect in mammalian cells. Mol Cell Biol 21:3436–3444
12. Chen C, Pore N, Behrooz A, Ismail-Beigi F, Maity A (2001) Regulation of glut1 mRNA by hypoxia-inducible factor-1. Interaction between H-ras and hypoxia. J Biol Chem 276:9519–9525
13. Harris AL (2002) Hypoxia—a key regulatory factor in tumour growth. Nat Rev Cancer 2:38–47
14. Weber G (1977) Enzymology of cancer cells (second of two parts). N Engl J Med 296:541–551
15. Weber G (1977) Enzymology of cancer cells (first of two parts). N Engl J Med 296:486–492
16. Younes M, Brown RW, Stephenson M, Gondo M, Cagle PT (1997) Overexpression of Glut1 and Glut3 in stage I nonsmall cell lung carcinoma is associated with poor survival. Cancer 80:1046–1051
17. Younes M, Brown RW, Mody DR, Fernandez L, Laucirica R (1995) GLUT1 expression in human breast carcinoma: correlation with known prognostic markers. Anticancer Res 15:2895–2898
18. Gambhir SS (2002) Molecular imaging of cancer with positron emission tomography. Nat Rev Cancer 2:683–693
19. Haberkorn U, Morr I, Oberdorfer F, Bellemann ME, Blatter J, Altmann A, Kahn B, van Kaick G (1994) Fluorodeoxyglucose uptake in vitro: aspects of method and effects of treatment with gemcitabine. J Nucl Med 35:1842–1850
20. Haberkorn U, Ziegler SI, Oberdorfer F, Trojan H, Haag D, Peschke P, Berger MR, Altmann A, van Kaick G (1994) FDG uptake, tumor proliferation and expression of glycolysis associated genes in animal tumor models. Nucl Med Biol 21:827–834
21. Burt BM, Humm JL, Kooby DA, Squire OD, Mastorides S, Larson SM, Fong Y (2001) Using positron emission tomography with [(18)F]FDG to predict tumor behavior in experimental colorectal cancer. Neoplasia 3:189–195
22. Waki A, Fujibayashi Y, Magata Y, Yokoyama A, Sadato N, Tsuchida T, Ishii Y, Yonekura Y (1998) Glucose transporter protein-independent tumor cell accumulation of fluorine-18-AFDG, a lipophilic fluorine-18-FDG analog. J Nucl Med 39:245–250
23. Younes M, Lechago LV, Somoano JR, Mosharaf M, Lechago J (1996) Wide expression of the human erythrocyte glucose transporter Glut1 in human cancers. Cancer Res 56:1164–1167
24. Hanahan D (1985) Heritable formation of pancreatic beta-cell tumours in transgenic mice expressing recombinant insulin/simian virus 40 oncogenes. Nature 315:115–122
25. Folkman J, Watson K, Ingber D, Hanahan D (1989) Induction of angiogenesis during the transition from hyperplasia to neoplasia. Nature 339:58–61
26. Bergers G, Javaherian K, Lo KM, Folkman J, Hanahan D (1999) Effects of angiogenesis inhibitors on multistage carcinogenesis in mice. Science 284:808–812
27. Schaffhauser B, Veikkola T, Strittmatter K, Antoniadis H, Alitalo K, Christofori G (2006) Moderate antiangiogenic activity by local, transgenic expression of endostatin in Rip1Tag2 transgenic mice. J Leukoc Biol 80:669–676

28. Alfke H, Kohle S, Maurer E, Celik I, Rascher-Friesenhausen R, Behrens S, Heverhagen JT, Peitgen HO, Klose KJ (2004) Analysis of mice tumor models using dynamic MRI data and a dedicated software platform*. Rofo 176:1226–1231
29. Hellwig D, Menges M, Schneider G, Moellers MO, Romeike BF, Menger MD, Kirsch CM, Samnick S (2005) Radioiodinated phenylalanine derivatives to image pancreatic cancer: a comparative study with [18F]fluoro-2-deoxy-D-glucose in human pancreatic carcinoma xenografts and in inflammation models. Nucl Med Biol 32:137–145
30. Medarova Z, Pham W, Kim Y, Dai G, Moore A (2006) In vivo imaging of tumor response to therapy using a dual-modality imaging strategy. Int J Cancer 118:2796–2802
31. Bouvet M, Spernyak J, Katz MH, Mazurchuk RV, Takimoto S, Bernacki R, Rustum YM, Moossa AR, Hoffman RM (2005) High correlation of whole-body red fluorescent protein imaging and magnetic resonance imaging on an orthotopic model of pancreatic cancer. Cancer Res 65:9829–9833
32. Wild D, Behe M, Wicki A, Storch D, Waser B, Gotthardt M, Keil B, Christofori G, Reubi JC, Macke HR (2006) [Lys40(Ahx-DTPA-111In)NH2]exendin-4, a very promising ligand for glucagon-like peptide-1 (GLP-1) receptor targeting. J Nucl Med 47:2025–2033
33. Speiser DE, Miranda R, Zakarian A, Bachmann MF, McKall-Faienza K, Odermatt B, Hanahan D, Zinkernagel RM, Ohashi PS (1997) Self antigens expressed by solid tumors Do not efficiently stimulate naive or activated T cells: implications for immunotherapy. J Exp Med 186:645–653
34. De Lott LB, Morrison C, Suster S, Cohn DE, Frankel WL (2005) CDX2 is a useful marker of intestinal-type differentiation: a tissue microarray-based study of 629 tumors from various sites. Arch Pathol Lab Med 129:1100–1105
35. Nozawa H, Chiu C, Hanahan D (2006) Infiltrating neutrophils mediate the initial angiogenic switch in a mouse model of multistage carcinogenesis. Proc Natl Acad Sci U S A 103:12493–12498
36. Inoue M, Hager JH, Ferrara N, Gerber HP, Hanahan D (2002) VEGF-A has a critical, nonredundant role in angiogenic switching and pancreatic beta cell carcinogenesis. Cancer Cell 1:193–202
37. Berlin JD, Catalano P, Thomas JP, Kugler JW, Haller DG, Benson AB 3rd (2002) Phase III study of gemcitabine in combination with fluorouracil versus gemcitabine alone in patients with advanced pancreatic carcinoma: Eastern Cooperative Oncology Group Trial E2297. J Clin Oncol 20:3270–3275
38. Colucci G, Giuliani F, Gebbia V, Biglietto M, Rabitti P, Uomo G, Cigolari S, Testa A, Maiello E, Lopez M (2002) Gemcitabine alone or with cisplatin for the treatment of patients with locally advanced and/or metastatic pancreatic carcinoma: a prospective, randomized phase III study of the Gruppo Oncologia dell'Italia Meridionale. Cancer 94:902–910
39. Kindler HL, Friberg G, Singh DA, Locker G, Nattam S, Kozloff M, Taber DA, Karrison T, Dachman A, Stadler WM, Vokes EE (2005) Phase II trial of bevacizumab plus gemcitabine in patients with advanced pancreatic cancer. J Clin Oncol 23:8033–8040
40. Shibaji T, Nagao M, Ikeda N, Kanehiro H, Hisanaga M, Ko S, Fukumoto A, Nakajima Y (2003) Prognostic significance of HIF-1 alpha overexpression in human pancreatic cancer. Anticancer Res 23:4721–4727
41. Ogata M, Naito Z, Tanaka S, Moriyama Y, Asano G (2000) Overexpression and localization of heat shock proteins mRNA in pancreatic carcinoma. J Nippon Med Sch 67:177–185
42. Baker CH, Solorzano CC, Fidler IJ (2002) Blockade of vascular endothelial growth factor receptor and epidermal growth factor receptor signaling for therapy of metastatic human pancreatic cancer. Cancer Res 62:1996–2003
43. Bruns CJ, Solorzano CC, Harbison MT, Ozawa S, Tsan R, Fan D, Abbruzzese J, Traxler P, Buchdunger E, Radinsky R, Fidler IJ (2000) Blockade of the epidermal growth factor receptor signaling by a novel tyrosine kinase inhibitor leads to apoptosis of endothelial cells and therapy of human pancreatic carcinoma. Cancer Res 60:2926–2935
44. Yamanaka Y, Friess H, Kobrin MS, Buchler M, Beger HG, Korc M (1993) Coexpression of epidermal growth factor receptor and ligands in human pancreatic cancer is associated with enhanced tumor aggressiveness. Anticancer Res 13:565–569
45. Sanderson S, Valenti M, Gowan S, Patterson L, Ahmad Z, Workman P, Eccles SA (2006) Benzoquinone ansamycin heat shock protein 90 inhibitors modulate multiple functions required for tumor angiogenesis. Mol Cancer Ther 5:522–532
46. Sebastian S, Kenkare UW (1998) Expression of two type II-like tumor hexokinase RNA transcripts in cancer cell lines. Tumor Biol 19:253–260
47. Rasschaert J, Malaisse WJ (1995) Activity of cytosolic and mitochondrial enzymes participating in nutrient catabolism of normal and tumoral islet cells. Int J Biochem Cell Biol 27:195–200
48. Therasse P, Arbuck SG, Eisenhauer EA, Wanders J, Kaplan RS, Rubinstein L, Verweij J, Van Glabbeke M, van Oosterom AT, Christian MC, Gwyther SG (2000) New guidelines to evaluate the response to treatment in solid tumors. European Organization for Research and Treatment of Cancer, National Cancer Institute of the United States, National Cancer Institute of Canada. J Natl Cancer Inst 92:205–216